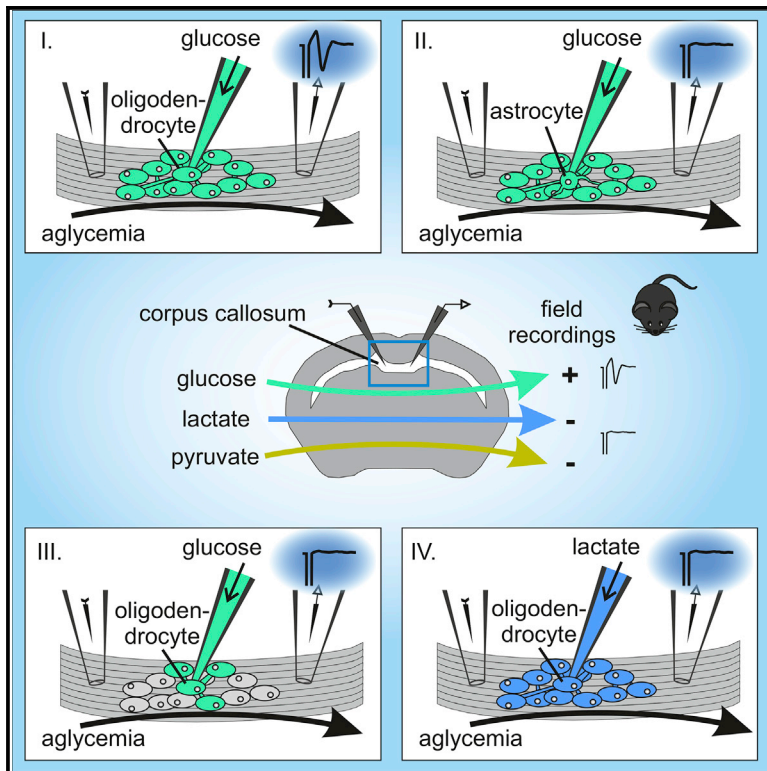


Oligodendrocytes in the Mouse Corpus Callosum Maintain Axonal Function by Delivery of Glucose

Graphical Abstract



Authors

Niklas Meyer, Nadine Richter, Zoya Fan, ..., Marcus Semtner, Christiane Nolte, Helmut Kettenmann

Correspondence

kettenmann@mdc-berlin.de

In Brief

Meyer et al. find that, unlike in the optic nerve, lactate does not substitute for glucose to sustain axonal function in the mouse corpus callosum. Oligodendrocyte networks in the corpus callosum provide energy substrates to axons predominantly by delivery of glucose, indicating different metabolic support mechanisms among white matter regions.

Highlights

- Aglycemia abolishes compound action potentials (CAPs) in the corpus callosum
- Lactate perfusion is unable to rescue callosal CAPs during aglycemia
- Filling single oligodendrocytes with glucose rescues axonal function during aglycemia
- Coupled glial networks are a prerequisite for this rescue



Oligodendrocytes in the Mouse Corpus Callosum Maintain Axonal Function by Delivery of Glucose

Niklas Meyer,¹ Nadine Richter,^{1,3} Zoya Fan,^{1,4} Gabrielle Siemonsmeier,¹ Tatyana Pivneva,⁵ Philipp Jordan,¹ Christian Steinhäuser,² Marcus Semtner,¹ Christiane Nolte,¹ and Helmut Kettenmann^{1,6,*}

¹Cellular Neurosciences, Max Delbrueck Center for Molecular Medicine in the Helmholtz Association, Robert Roessle Str. 10, 13125 Berlin, Germany

²Institute of Cellular Neurosciences, Medical Faculty, University of Bonn, Sigmund Freud Str. 25, 53105 Bonn, Germany

³Inspire Medical Systems, Inc., 9700 63rd Ave N, Suite 200, Maple Grove, MN 55369, USA

⁴Department of Biology, Massachusetts Institute of Technology, 77 Massachusetts Ave., Cambridge, MA 02139, USA

⁵Bogomoletz Institute of Physiology, Department of Sensory Signaling, 01024 Kiev, Ukraine

⁶Lead Contact

*Correspondence: kettenmann@mdc-berlin.de

<https://doi.org/10.1016/j.celrep.2018.02.022>

SUMMARY

In the optic nerve, oligodendrocytes maintain axonal function by supplying lactate as an energy substrate. Here, we report that, in acute brain slices of the mouse corpus callosum, exogenous glucose deprivation (EGD) abolished compound action potentials (CAPs), which neither lactate nor pyruvate could prevent. Loading an oligodendrocyte with 20 mM glucose using a patch pipette prevented EGD-mediated CAP reduction in about 70% of experiments. Loading oligodendrocytes with lactate rescued CAPs less efficiently than glucose. In mice lacking connexin 47, oligodendrocyte filling with glucose did not prevent CAP loss, emphasizing the importance of glial networks for axonal energy supply. Compared with the optic nerve, the astrocyte network in the corpus callosum was less dense, and loading astrocytes with glucose did not prevent CAP loss during EGD. We suggest that callosal oligodendrocyte networks provide energy to sustain axonal function predominantly by glucose delivery, and mechanisms of metabolic support vary across different white matter regions.

INTRODUCTION

In white matter, oligodendrocytes are instrumental to fuel axonal activity, and the optic nerve has served as a convenient model to study the mechanism of this cellular interaction (Morrison et al., 2013). Metabolites and signaling molecules can pass from the oligodendrocyte soma through cytoplasm-rich myelinic channels in the compacted myelin to the innermost tips of the oligodendrocyte process enwrapping an axon. Evidence for axon-oligodendrocyte metabolic coupling initially came from studies of optic nerve explants that were subjected to glucose deprivation (Fünfschilling et al., 2012; Lee et al., 2012; Morrison et al., 2013; Simons and Nave, 2015). Lactate

is considered to be the energy metabolite delivered by oligodendrocytes. Indeed, compound action potentials (CAPs) can be evoked in acutely isolated optic nerve preparations and can persist for several hours but rapidly fail under aglycemic conditions. This failure can be effectively prevented by perfusion of L-lactate (Brown et al., 2003). On the basis of these studies, it has been proposed that axons are at least partly powered by lactate (or pyruvate) provided by oligodendrocytes. Lactate is released into the periaxonal space by the monocarboxylate transporter 1 (MCT1), which is strongly expressed by oligodendrocytes (Fünfschilling et al., 2012; Lee et al., 2012). Lactate can then be taken up by axons via the neuronal isoform MCT2 for mitochondrial ATP production. Recently, Saab et al. (2016) demonstrated that NMDA receptors on oligodendrocytes play a key role in controlling the metabolic cooperation between oligodendrocytes and axons. In the optic nerve, NMDA receptor activation in response to glutamate release increases trafficking of glucose transporter GLUT1 to the oligodendrocyte membrane, thus sustaining glucose import to oligodendrocytes for glycolysis and downstream transfer of lactate to axons. This mechanism might be important in diseases linked to energy deprivation (e.g., white matter ischemia).

Intact gap junctional coupling among glial cells is a prerequisite for myelin maintenance and axonal function (Tress et al., 2011, 2012). According to the current concept, astrocytes transfer energy substrates from the vasculature, convert it to lactate, and pass it to oligodendrocytes via gap junctions (Nave and Werner, 2014). It is also conceivable that astrocytes directly fuel axons, as their processes protrude into nodes of Ranvier. Gap junctions are integral membrane structures consisting of connexins, which allow diffusion of ions, signaling molecules, and metabolites of up to 1 kDa, including glucose or lactate. In the corpus callosum, oligodendrocytes and astrocytes exhibit panglial coupling via connexin isoforms Cx30 and Cx43, expressed by astrocytes, and Cx32 and Cx47, expressed by oligodendrocytes. Cx47 ablation completely abolishes coupling of oligodendrocytes to astrocytes and results in smaller oligodendrocyte networks (Maglione et al., 2010).



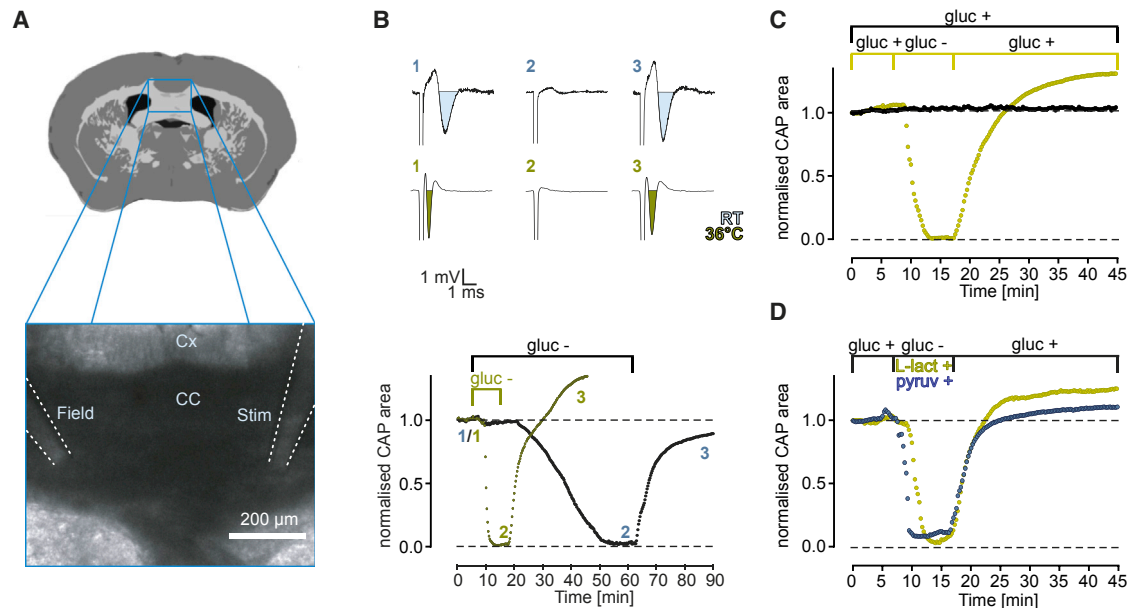


Figure 1. Exogenous Glucose Deprivation Leads to Rapid Decline of Axonal Activity in the Corpus Callosum

(A) Overview of a frontal brain slice used for electrophysiological recordings. The inset shows the position of the field (Field) and stimulation (Stim) electrodes. Evoked CAPs were measured by the field electrode. CC, corpus callosum; Cx, cortex.

(B) Representative recordings of CAPs to illustrate the time course of CAP decline during 55 min (at room temperature) or 10 min (at 36°C) EGD (gluc-). The sample traces for experiments at room temperature (top, blue) and 36°C (green) show the CAPs at the beginning of the experiment (1), during EGD (2), and after glucose was reperused (3). The filled area (blue/green) corresponds to the area for CAP calculation. Plots at the bottom show sample traces of normalized CAP areas during glucose deprivation and reperfusion.

(C) Representative traces for CAP progression at 36°C with (green) and without (black) a 10 min EGD period. An overshoot of the CAPs is apparent after EGD ($n = 4$, $N = 1$).

(D) Representative CAP traces (36°C) in which glucose was replaced by either 20 mM L-lactate or 20 mM pyruvate during a 10 min EGD period. CAPs cannot be maintained during glucose deprivation by equimolar amounts of lactate or pyruvate.

Although the optic nerve has served as a model for most previous studies to analyze oligodendrocyte-axonal metabolic coupling, we have now studied another white matter structure, the corpus callosum. As the largest white matter structure in the brain, it connects the left and right cerebral hemispheres and enables interhemispheric communication. In contrast to the optic nerve, which is completely myelinated, the corpus callosum contains only about 30%–40% of myelinated fibers and thus exhibits a different architecture (Mack et al., 1995). The present study was prompted by our initial observation that the perfusion of L-lactate is not sufficient to preserve axonal activity in the corpus callosum during exogenous glucose deprivation (EGD). This was in contrast to the findings in optic nerve (Brown et al., 2003, 2005), which implies distinct mechanisms of neuron-glia cooperation in different white matter regions. We adapted an approach originally used to investigate how astrocytes provide energy substrates to neurons in gray matter. Rouach et al. (2008) showed that intracellular application of glucose or lactate into hippocampal astrocytes sustains glutamatergic synaptic transmission during exogenous glucose deprivation. Here, we filled glucose or lactate into oligodendrocytes or astrocytes in the corpus callosum and found that the most efficient combination to maintain axonal activity during glucose deprivation was the delivery of glucose into oligodendrocytes.

RESULTS

CAPs Quickly Decline under Exogenous Glucose Deprivation, and This Decline Is Not Prevented by Adding Lactate or Pyruvate

To monitor axonal function in the corpus callosum under normal and aglycemic conditions, stimulation and recording electrodes were placed in freshly prepared coronal brain slices, as shown in Figure 1A. Twenty-five pulses at a frequency of 50 Hz were applied every 15 s (0.5 s stimulation and 14.5 s recovery time), and CAPs were recorded. For quantification, we determined the area under the action potential curve (i.e., integral of amplitude over time), which reflects the number of active axons and the magnitude of the individual action potentials. CAP amplitudes remained constant over recording periods of at least 45 min in continuously gassed (95% O₂, 5% CO₂) artificial cerebrospinal fluid (ACSF) containing 10 mM glucose at 36°C (Figure 1C, black trace). CAPs were dependent on voltage-gated Na⁺ channels, as application of tetrodotoxin (TTX) (1 μM) completely blocked them (Figure S1). For aglycemia experiments, we recorded CAPs for 5 min in normal ACSF and subsequently changed to glucose-free ACSF for 10 min. CAP amplitudes declined within 5 min to almost zero and remained at this level in all experiments ($n = 37$) during exogenous glucose deprivation (EGD). Upon reapplication of 10 mM glucose, CAP

amplitudes recovered to their initial value within 5 min. In most experiments, the CAP amplitudes showed an overshoot of 110%–150% (Figure 1C, green). We also performed experiments at room temperature to test the impact of temperature on metabolic activity. CAP activity declined considerably more slowly in glucose-free solution and reached a steady state close to zero only after about 30 min. The slice was maintained in glucose-free solution for 55 min. Upon reperfusion of glucose-containing ACSF, CAP activity recovered to baseline within 20 min and, in contrast to recordings at 36°C (green), did not overshoot (Figure 1B, black trace).

We next tested if lactate or pyruvate can sustain CAP activity during aglycemia, as observed in the optic nerve (Brown et al., 2003). When we replaced 10 mM glucose with 20 mM L-lactate, CAP activity declined as rapidly as in glucose-free solution and recovered only by reperfusion of glucose (Figure 1D, green). Replacement of 10 mM glucose with 20 mM pyruvate also resulted in a rapid decline of CAP activity and showed recovery only after glucose reperfusion (Figure 1D, blue trace). These findings indicate that glucose specifically, rather than lactate or pyruvate, is required to maintain axonal activity in the corpus callosum in this experimental paradigm.

Loss of CAPs during EGD Can Be Prevented by Loading Glucose into Single Oligodendrocytes

We tested whether glucose supply from oligodendrocytes could compensate for the depletion of glucose in the ACSF. Oligodendrocytes in acute brain slices from PLP-GFPxhGFAP-mRFP transgenic mice were identified by their GFP fluorescence and astrocytes by their mRFP fluorescence (Hirrlinger et al., 2005). An oligodendrocyte in the corpus callosum was patch-clamped and dialyzed for 20 min with intracellular solution containing 20 mM glucose prior to the CAP recordings and the induction of EGD. The intracellular solution also contained the fluorescent dye Sulforhodamine B to verify successful dialysis of the cell. The injected cells were further characterized by recording their membrane currents at a holding potential of -70 mV and during de- and hyperpolarizing voltage steps. The cells typically showed some current decay during the voltage step and large symmetrical tail currents, a characteristic feature of mature oligodendrocytes (Berger et al., 1991) (Figure 2B). The patched oligodendrocytes had an average input resistance of 62.59 ± 5.67 M Ω , a reversal potential of -64.34 ± 1.97 mV, and a membrane capacitance of 23.09 ± 3.35 pF ($n = 22$, $N = 17$). These properties did not significantly change in the course of the 20 min dialysis (Figure 2B), indicating that network composition was not altered. After dialysis of an oligodendrocyte with 20 mM glucose, we measured CAP activity during EGD, as described above. In about 70% of the experiments, the fast EGD-induced drop of CAP activity was not seen when oligodendrocytes had been pre-loaded with glucose, and the normalized CAP amplitude shortly before reperfusion (at 16 min) was on average still $43\% \pm 8.1\%$ of the maximum CAP amplitude ($n = 14$, $N = 10$; includes those experiments in which the CAP value at 16 min was still $\geq 30\%$ of the maximal CAP value). The averaged traces for CAP activity during EGD in control and after dialysis of an oligodendrocyte with glucose are shown in Figure 2A. The scatterplot at the bottom shows the normalized CAP amplitudes at

16 min for each experiment, shortly before reperfusion with normal ACSF. It is apparent that the extent of CAP maintenance during EGD after oligodendrocyte loading varies, possibly because of the size of the associated panglial network. To control for unspecific loading effects, we used the non-metabolizable sugar mannitol instead of glucose for dialysis prior to EGD. In none of the experiments could mannitol prevent the loss of CAPs during EGD (Figure 5B; $n = 6$). In conclusion, elevated glucose in oligodendrocytes can prevent the loss of CAPs during EGD.

Loading Single Astrocytes with Glucose Was Much Less Effective in Preventing CAP Loss during EGD

In a similar approach as described above, we dialyzed astrocytes with 20 mM glucose. The astrocytes, identified by their red fluorescent transgene expression, typically displayed an average input resistance of 45.51 ± 10.47 M Ω , a reversal potential of -78.67 ± 1.80 mV, and a membrane capacitance of 16.31 ± 8.90 pF ($n = 4$, $N = 4$). Similar to the oligodendrocytes, passive membrane properties did not significantly change in the course of the 20 min dialysis (Figure 2B). In contrast to dialyzing oligodendrocytes with 20 mM glucose, loading of astrocytes did not significantly influence CAP decline during EGD; a partial rescue of CAP activity during EGD was observed in only one of ten experiments (Figure 2A; $n = 10$, $N = 6$, $p = 0.245$).

It has been reported that slightly elevated extracellular K^+ concentrations ($[K^+]_e$) can stimulate astrocytic glucose consumption, glycogen mobilization, and lactate depletion from astrocytes in tissue slices (Hof et al., 1988; Sotelo-Hitschfeld et al., 2015). We therefore repeated the experiments in a bathing solution with $[K^+]_e$ lowered from 5 to 2.5 mM. In only two of ten experiments, there was a moderate prevention of CAP loss during EGD after astrocyte glucose loading, but the mean of the normalized CAP area during EGD did not significantly differ in comparison with experiments performed at elevated $[K^+]_e$ ($p = 0.201$; Figure S2).

Biocytin Injection into Oligodendrocytes Mainly Spreads into a Network of Coupled Oligodendrocytes

The panglial network of astrocytes and oligodendrocytes in the corpus callosum has so far been characterized only in young (10–25 days old) mice (Maglione et al., 2010) but not in older mice as used in our study. We analyzed the extent of coupling in 18 slices from five animals (28–35 days old). PLP-GFP-expressing oligodendrocytes close to the midline in the corpus callosum (Figure 3) were dialyzed with a pipette solution containing biocytin for 20 min. Slices were subsequently fixed. In 16 of 18 slices, we found networks consisting of 22.5 ± 3.3 coupled cells on average, and the tracer spread up to 360 μ m along the longitudinal axis (195 ± 19 μ m, $n = 16$). For further characterization of the networks, Olig2 and GFAP antibodies were used to identify oligodendrocytes and astrocytes, respectively. Figure 3B (left column) shows a typical example of a coupled network that was filled via an oligodendrocyte. The biocytin-Cy3-stained cells had the typical morphology of oligodendrocytes, with their cell bodies arranged like a “rope of pearls” and their processes aligned in parallel with axons. The networks were usually oval shaped, with the longitudinal axis oriented in parallel to the

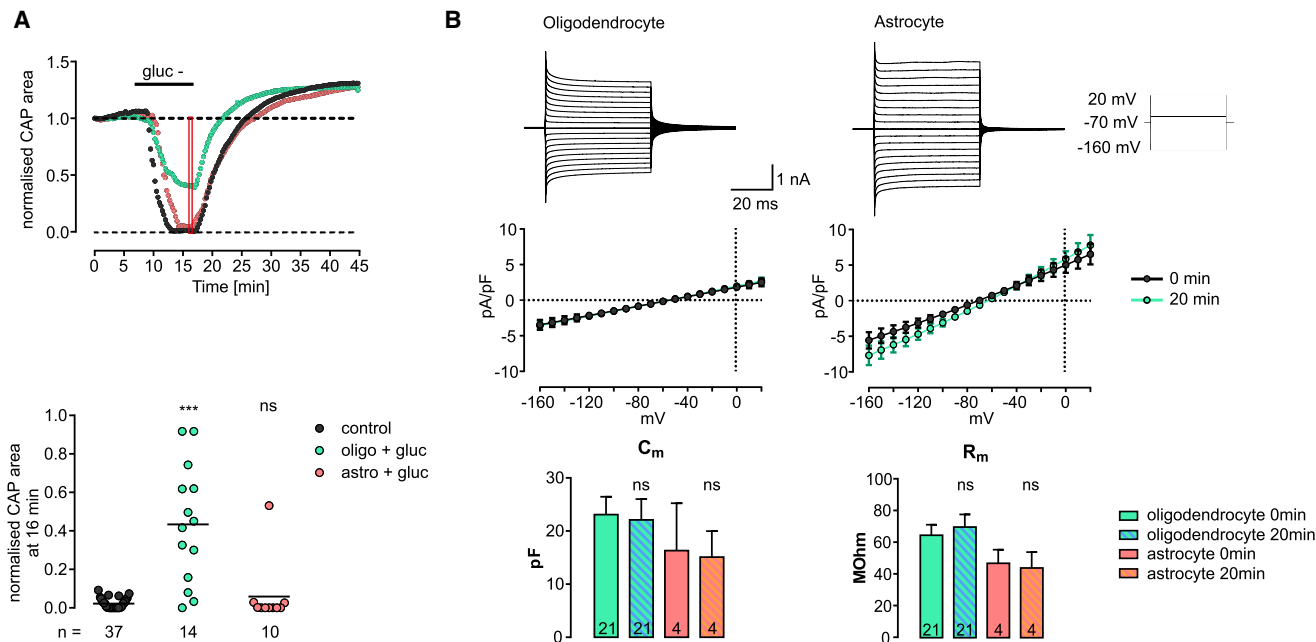


Figure 2. Glucose Loading of Oligodendrocytes but Not of Astrocytes Can Sustain Axonal Firing during EGD

GFP-positive oligodendrocytes or mRFP-positive astrocytes in the corpus callosum of a PLP-GFPxhGFAP-RFP transgenic mouse were preloaded with 20 mM glucose before recording of CAPs.

(A) Top: averaged traces for CAP progression during 10 min EGD (glut-) and reperfusion at 36°C without (black) or with preloading of glucose in an oligodendrocyte (green) or astrocyte (red). Bottom: scatterplot illustrates the normalized CAP areas at 16 min (as indicated by the red square in the top graph), shortly before reperfusion with glucose-containing ACSF. Glucose loading via oligodendrocytes could significantly sustain CAPs during aglycemia, whereas glucose loading via astrocytes prevented CAP loss in one of ten experiments (control without preloading, n = 37, N = 23; oligodendrocytes + glucose, n = 14, N = 10; astrocytes + glucose, n = 10, N = 6; Kruskal-Wallis test, $p < 0.05$, black line represents the mean).

(B) The inset shows the typical current profile of an oligodendrocyte (left) and astrocyte (right) clamped at -70 mV in response to 10 de- and hyperpolarizing voltage steps. Only cells that displayed a series resistance of $\leq 125\%$ of the initial value after 20 min of dialysis were included for the following analysis. The graphs in the middle show the averaged current densities plotted against the corresponding voltages of both cell types at the start and the end of the 20 min dialysis period (black, 0 min; green, 20 min). The bottom graphs compare the membrane capacitance (C_m) and membrane resistance (R_m) of oligodendrocytes and astrocytes at the start and the end of the dialysis. No significant differences were observed in either comparison (oligodendrocyte, n = 21, N = 7; astrocyte, n = 4, N = 4; t test, $p > 0.05$). The number of experiments is indicated in the bars. Error bars reflect SEM.

axonal processes (Figure 3B). In some instances, the biocytin also traced the oligodendrocyte processes. Interestingly, the oligodendroglial markers labeled only a subpopulation of the coupled cells; Olig2, a transcription factor expressed by cells of the oligodendrocytic lineage (Trotter et al., 2010), labeled $34.8\% \pm 4.9\%$ (108 of 360) of biocytin-filled cells, and $35.1\% \pm 5.8\%$ (134 of 360) of the coupled cells expressed the PLP transgene. The two populations overlapped only partly (80 of 360 cells expressed both Olig2 and PLP-GFP). Nevertheless, because of their morphology and typical arrangement, we conclude that the networks consist mainly of oligodendrocytes. GFAP labeling was rarely found in the biocytin-positive cells, indicating that astrocytes were either excluded from the networks that were filled via an oligodendrocyte, or were not labeled by GFAP.

To obtain an approximate estimate of the ratio of oligodendrocytes to astrocytes at the midline region of the corpus callosum, we quantified PLP-positive and mRFP-positive cells, based on the intrinsic fluorescence of the two transgenes. We analyzed 15 coronal sections of anterior corpus callosum of N = 3 double-transgenic mice and found 59.8 ± 2.2 PLP-GFP-positive

cells and 7.6 ± 0.3 GFAP-mRFP-positive cells on average per given volume. This corresponds to a ratio of 88.7% oligodendrocytes and 11.3% astrocytes (Figure 3A). Although we are aware that the transgenes do not label the entire oligodendrocyte and astrocyte population (Fuss et al., 2000), and the mRFP transgene sometimes shows a mosaic-like expression pattern, our estimate is in the same range as reported for the anterior CC of rats (Reyes-Haro et al., 2013).

Because our observations suggest differences in astrocyte-axonal metabolic coupling in corpus callosum compared with optic nerve, we performed GFAP immunostaining in coronal sections of anterior corpus callosum and in longitudinal optic nerve sections to compare the density and cytoarchitecture of GFAP-positive structures. In the corpus callosum, GFAP-positive astrocytes are scattered throughout the tissue and appear as individual, fibrous-like cells with processes of irregular caliber traversing mostly parallel to the axons, with endfeet contacting the blood vessels (Figure 3E). In contrast, in the optic nerve GFAP immunolabeling reveals a dense network of processes that appear knotted and irregular in shape (Figure 3E) and confirm what Sun et al. (2009) reported for the optic nerve

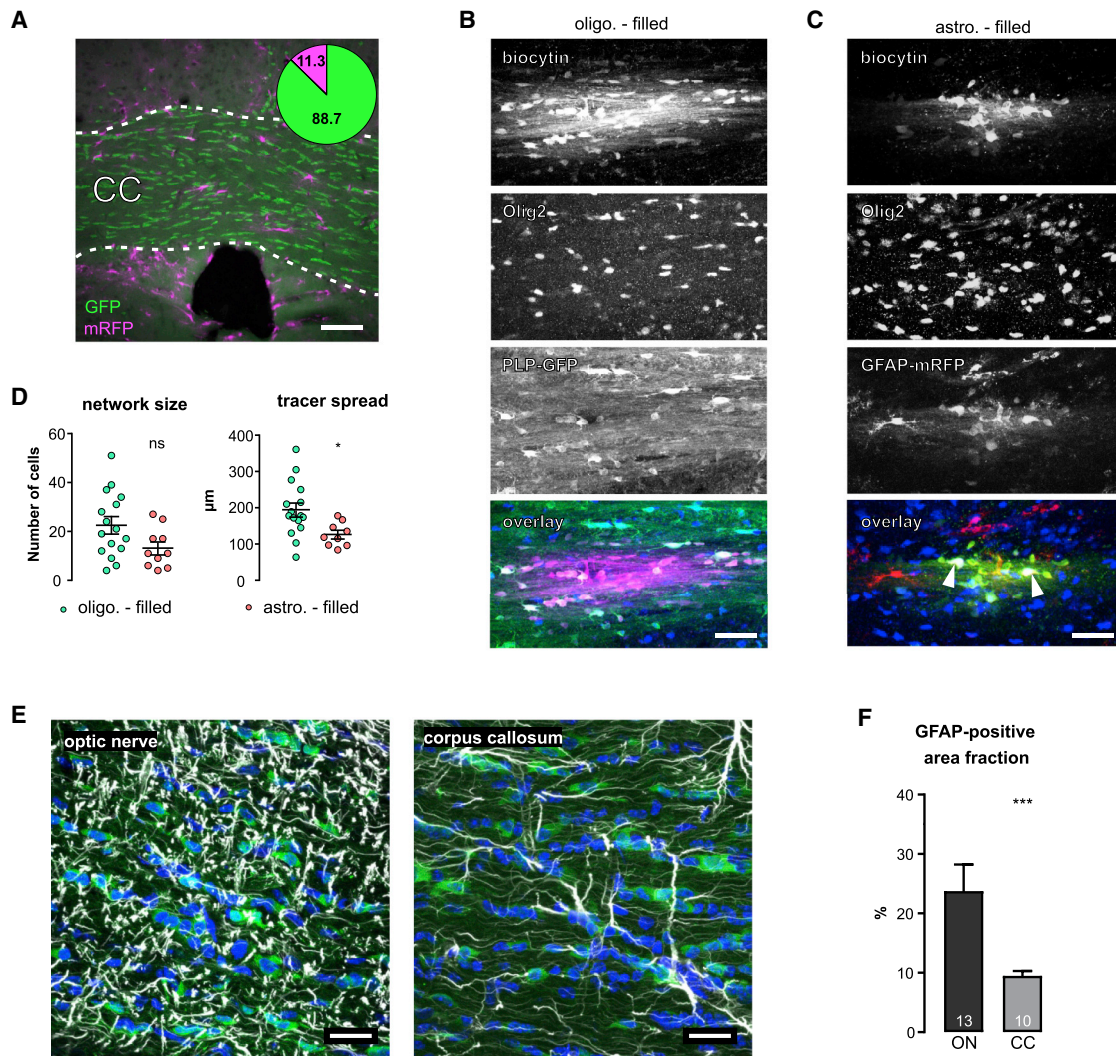


Figure 3. Appearance of Coupled Glial Networks in the Corpus Callosum and Difference in Astrocyte Density Compared with Optic Nerve

(A) Maximum intensity projection of a z stack of confocal images demonstrates the distribution of genetically labeled oligodendrocytes and astrocytes in the medial corpus callosum (CC) of a PLP-GFPxhGFAP-mRFP transgenic mouse. Bar denotes 100 μ m. Pie chart demonstrates the percentage of PLP-GFP-positive versus hGFAP-mRFP-positive cells in native coronal slices near the midline of the corpus callosum averaged from $n = 15$ slices with duplicate to triplicate values ($N = 3$).

(B) Projection of z stack images of a glial network filled with biocytin via an oligodendrocyte in a PLP-GFP transgenic mouse. Upper image shows biocytin visualized with streptavidin Cy3; below is an Olig2 staining of the same area and the PLP-GFP signal. In the merged image (overlay), biocytin is displayed in magenta; both PLP-GFP (green) and Olig2 (blue) are expressed only by a subpopulation of filled cells. Note the “rope of pearls” arrangement of the cell bodies; biocytin also fills oligodendrocyte processes running in parallel to axons. Bar denotes 50 μ m.

(C) Projection of z stack images of a glial network filled with biocytin via an astrocyte in a GFAP-mRFP mouse. Upper image shows biocytin visualized with streptavidin Cy2, below Olig2 staining of the same area, and the mRFP signal. In the overlay, biocytin is displayed in green, mRFP in red, and Olig2 in blue. The biocytin-filled network contains mRFP-expressing cells and Olig2-positive cells, cells expressing both markers (arrowheads), and cells expressing none of the markers. Bar denotes 50 μ m.

(D) Quantification of network size and horizontal spread of biocytin either filled via individual oligodendrocytes (green) or astrocytes (red) in transgenic animals as mentioned above. Network size is highly variable but on average not significantly smaller when filled via astrocytes; tracer does not spread as far when filled via astrocytes. $^*p < 0.05$ (Student’s two-tailed t test). In total we injected oligodendrocytes in 18 slices from $N = 5$ PLP-GFP transgenic mice and astrocytes in 12 slices from $N = 4$ GFAP-mRFP mice. Error bars reflect SEM.

(E) Coronal sections of anterior corpus callosum and longitudinal sections of the optic nerve were immunolabeled for GFAP (white). Projection images of 12 μ m z stacks show the cytoarchitecture and density of GFAP-positive structures. Green, PLP-GFP transgene expression; blue, DAPI. Bars denote 25 μ m. Error bars reflect SEM.

(F) Percentage area of coverage by GFAP was analyzed using ImageJ as described. Number indicates number of slices analyzed ($***p = 0.004$).

head. Astrocytic perikarya can hardly be recognized. For a quantitative comparison, we determined the area covered by GFAP-positive structures in projection images of 12- μ m-thick z stacks that had been obtained from labeled sections of six animals, using identical gain and offset settings. Projection images were binarized in ImageJ (without previous adjustments of contrast and brightness) by using identical thresholding settings for all images, and area coverage of GFAP-positive pixels was measured in five to six random frames per binarized image. In optic nerve sections ($n = 13$), the GFAP-covered area was $27.8\% \pm 2.9\%$ of the total area, while in corpus callosum sections ($n = 10$) it was only $9.5\% \pm 0.6\%$ ($p = 0.004$, two-tailed t test; [Figure 3F](#)), indicating a much higher density of GFAP-positive structures in the optic nerve.

Biocytin-Filled Astrocytes in the Corpus Callosum Couple to Astrocytes and Oligodendrocytes

When biocytin was loaded via mRFP-positive astrocytes, we also observed a large heterogeneity between the individual dye-filling experiments, with regard to both network size and tracer spread. However, on average, astroglial coupled networks tended to be more rotund, though spreading of the dye into longitudinal processes was observed as well. Filling via astrocytes ($n = 12$, $N = 4$) revealed coupled networks in ten slices, with 13.2 ± 2.5 coupled cells on average. However, the difference compared with the oligodendrocyte networks (see above) was not significant (Student's two-tailed t test, $p = 0.058$; [Figure 3D](#)). An example of a coupled network that was filled via an mRFP-positive astrocyte in the midline region of the corpus callosum of a GFAP-mRFP transgenic animal is shown in [Figure 3C](#). More than one quarter ($27.5\% \pm 4\%$) of the cells in the networks were immunolabeled for Olig2, whereas $44.4\% \pm 11.2\%$ (53 of 132 cells) of the biocytin-loaded cells expressed the transgene marker GFAP-mRFP. GFAP immunolabeling was found in 8% of the cells in the networks (not shown). We assume that mRFP-expressing cells within the filled networks are mostly astrocytes and that the number of astrocytes in the networks might rather be underestimated, as both the transgene and GFAP may not be expressed by all astrocytes, and the antibodies might not penetrate deeply enough to reach all biocytin-filled cells in deeper levels of the slice. The dye-loading experiments suggest that the networks, when loaded via an astrocyte, contain a higher proportion of astrocytes. Some cells in the networks are immunolabeled for Olig2, and biocytin diffuses into the longitudinal processes aligned with the axons, indicating that oligodendrocytes are also part of the network. The longitudinal extent of biocytin diffusion was smaller when astrocytes were dye-loaded ($126 \pm 11 \mu\text{m}$ compared with $195 \pm 19 \mu\text{m}$ in networks loaded via oligodendrocytes; Student's two-tailed t test, $p = 0.017$, [Figure 3D](#)). Surprisingly, about one third of the mRFP-positive cells (15 of 53) were also labeled for Olig2 ([Figure 3C](#), arrowhead). Cells with such unique immunohistochemical properties have been abundantly found in thalamic ganglionic networks ([Griemsmann et al., 2015](#)). In conclusion, regardless of whether they were filled via oligodendrocytes or astrocytes, the coupled glial networks in the corpus callosum of mice aged 28–35 days are heterogeneous in size, as reported before for younger animals ([Maglione et al., 2010](#)).

Glucose Loading of Oligodendrocytes in Cx47 Knockout Mice Does Not Prevent CAP Loss during EGD

To assess if inter-oligodendrocyte coupling is important for trafficking of glucose and metabolic support of axons, we used the Cx47-deficient mouse line, in which the size of coupled oligodendrocyte networks is markedly reduced, as shown for mice aged 10–15 days ([Maglione et al., 2010](#)). Oligodendrocytes were identified by their green fluorescence, as the Cx47-coding region was replaced by the cDNA encoding EGFP ([Odermatt et al., 2003](#)). Dialysis of 20 mM glucose into oligodendrocytes for 20 min could prevent CAP loss during EGD in none of the experiments in Cx47 knockout (Cx47KO) animals, and the mean of the normalized CAP area at 16 min did not differ significantly in comparison with the control ([Figure 4A](#); control 0.114 ± 0.058 , oligodendrocyte filling 0.141 ± 0.046 , $n = 8$ each, $N = 5$ animals each, $p = 0.902$). The passive membrane properties of oligodendrocytes in the Cx47KO mice did not significantly change in the course of the 20 min dialysis, indicating that the network composition was not altered ([Figure 4B](#)). Dye-filling experiments of slices from Cx47KO mice revealed significantly smaller coupled networks regarding the number of coupled cells (12.7 ± 2.2 versus 22.5 ± 3.3 in wild-type, $p = 0.048$). In Cx47KO animals, 29% of injected oligodendrocytes did not show any dye spread to adjacent cells (compared with 11% in wild-type). The tracer spread along the longitudinal axis was on average significantly smaller in Cx47KO animals ($112 \pm 20 \mu\text{m}$, $n = 12$, $N = 6$ animals) compared with wild-type ($195 \pm 19 \mu\text{m}$, $n = 16$, $N = 5$; $p = 0.0059$ in two-tailed t test; [Figures 4C and 4D](#)).

CAP Activity Can Partly Be Rescued by Dialysis of Oligodendrocytes with 40 mM L-Lactate during EGD

We next tested whether lactate can also generate a rescue effect when loaded into an oligodendrocyte prior to EGD. Interestingly, dialysis with 20 mM L-lactate did not significantly affect the loss of CAP activity during EGD. We next infused 40 mM lactate, because one glucose molecule can generate two molecules of lactate, and observed a partial prevention of the CAP decline during aglycemia ([Figure 5](#)). Although the effect was not as strong as that achieved by glucose, after loading 40 mM lactate, there was still some CAP activity left at 16 min compared with the control without preloading any metabolite. Mean values of the normalized CAP area were 0.119 ± 0.028 for 40 mM L-lactate ($n = 14$, $N = 7$) and 0.021 ± 0.004 for control ($n = 37$, $N = 23$, $p = 0.024$). Preloading with 20 mM mannitol, 20 mM L-lactate, or 20 or 40 mM pyruvate did not affect the CAP decline during 10 min EGD. As a negative control, non-metabolizable D-lactate (20 mM) also did not prevent CAP loss. The passive membrane properties of oligodendrocytes during and after clamping and during dialysis of intracellular solution with 40 mM L-lactate were not significantly altered by the procedure ([Figure S4](#)). As a control, dye-filling experiments of oligodendrocytes with intracellular solution containing 40 mM L-lactate or 10 mM glucose (equimolar to external glucose concentrations) did not reveal significant differences in the average number of coupled cells and dye spread, indicating that neither the high intracellular lactate nor the increased glucose concentration affect coupling and the size of glial networks as quantified by our method ([Figures S3 and S5](#)). In summary, although infusion of high lactate into

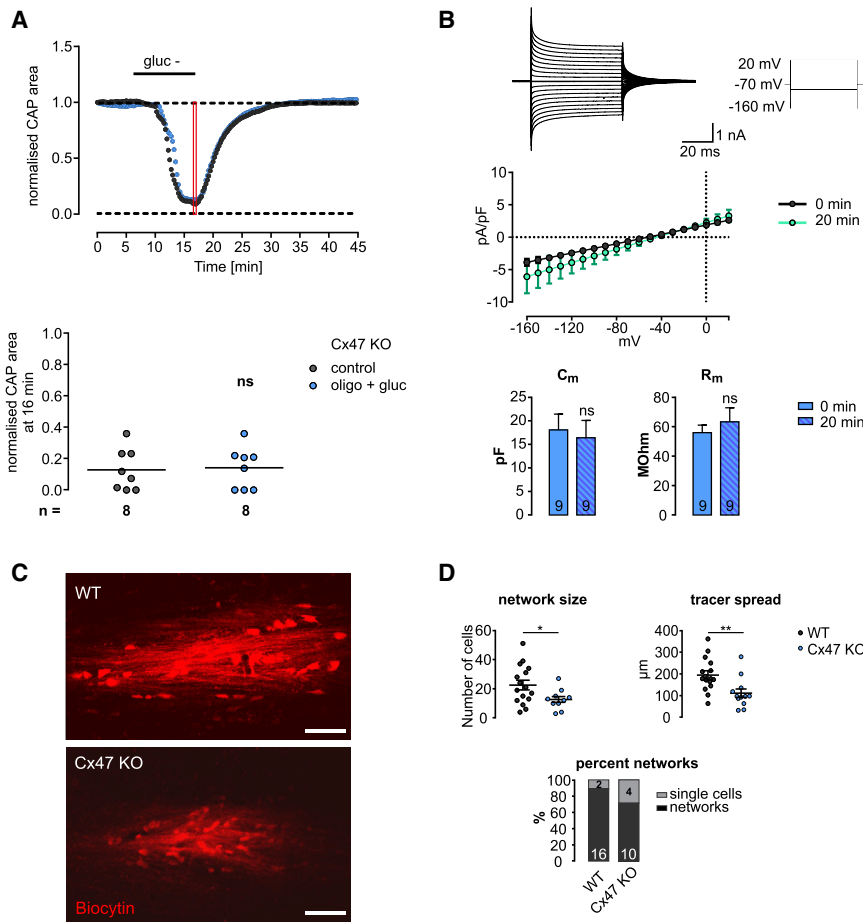


Figure 4. Glucose Loading of Oligodendrocytes in Cx47KO Mice Cannot Sustain Axonal Firing during EGD

Oligodendrocytes in the corpus callosum of Cx47KO transgenic mice were preloaded with 20 mM glucose before recording CAPs as described.

(A) Top: averaged traces for CAP progression during 10 min of EGD (gluc-) and reperfusion at 36°C without (black) or with preloading of oligodendrocytes (blue). Bottom: scatterplot of normalized CAP area at 16 min (as indicated in the top graphic) shortly before reperfusion. The CAP loss cannot be prevented by dialyzing oligodendrocytes with glucose in this mouse line (n = 8 experiments, N = 6, for control or 20 mM glucose; Kruskal-Wallis test, p > 0.05, black line represents the mean).

(B) The top panel shows the typical current profile of an oligodendrocyte clamped at -70 mV (left) in response to 10 de- and hyperpolarizing voltage steps (right) in a slice from a Cx47KO mouse. The graph in the middle shows the averaged current densities plotted against the corresponding voltages at the start and the end of the 20 min dialysis (black, 0 min; green, 20 min). No significant differences were observed at any given voltage step. The bottom graphs compare the membrane capacitance (C_m) and membrane resistance (R_m) of oligodendrocytes at the start and the end of the dialysis, respectively. No significant differences were observed in either comparison (t test, p > 0.05). The number of experiments is indicated at the bottom of the bar graphs (n = 9, N = 5 for each condition). Error bars reflect SEM.

(C) Examples of glial coupled networks (maximum intensity projection of z stacks of confocal images) after filling an oligodendrocyte with biocytin from wild-type (WT) or Cx47KO mice. Bar denotes 50 μm.

(D) Quantification of glial networks. Scatterplots show average number of coupled cells in networks from Cx47KO mice compared with WT (*p = 0.0418, t test). Average tracer spread as defined by the largest distance between two somata of the coupled network (**p = 0.0059, t test). Percentage of coupled networks observed in wild-type and Cx47KO mice. We analyzed n = 18, N = 5 wild-type, and n = 14 slices, N = 6 Cx47KO mice. Error bars reflect SEM.

oligodendrocytes can partially prevent the loss of CAPs, glucose filling was most efficient.

Simultaneous Disruption of Both Glucose and Monocarboxylate Transport Inhibits the Prevention of CAP Loss Seen after Glucose Loading of Oligodendrocytes

To further characterize the mechanisms involved in the prevention of EGD-induced CAP loss due to preloading of glucose into oligodendrocyte networks, we tested the effect of inhibited metabolite transport. We blocked MCTs, which are able to transport monocarboxylates, using 4-CIN (α-cyano-4-hydroxycinnamic acid; 200 μM) or AR-C155858 (1 μM). The latter specifically inhibits MCT1 and MCT2, the isoforms expressed by oligodendrocytes and neurons, respectively, whereas 4-CIN acts on all MCT subtypes. We also used Stf31 to inhibit glucose transporter GLUT1, which is specifically expressed by oligodendrocytes and astrocytes, and GTI2, which specifically blocks GLUT3 on axons. Ten minute application of 4-CIN, AR-C155858, or Stf31 in the presence of external glucose did not significantly alter CAPs (not shown). The combined applica-

tion of AR-C155858 and Stf31 or the single application of GTI2 lead to a moderate drop of CAPs of about 20% during the application period (Figure 6A). We then studied the effect of the inhibitors on the CAP decline during EGD after filling an oligodendrocyte with glucose. 4-CIN significantly reduced the CAP amplitudes and thus abolished the rescue effect of glucose dialysis (n = 11, N = 5). AR-C155858 (n = 9, N = 4) and Stf31 (n = 17, N = 9) alone did not significantly affect the prevention of CAP loss. A combined application of AR-C155858 and Stf31 or the application of GTI2, however, completely abolished the effect of glucose loading on CAP loss; CAPs dropped as in the control without preloading glucose into oligodendrocytes (AR-C155858 and Stf31, n = 13, N = 5 animals; GTI2, n = 5, N = 2 animals; Figure 6B). Thus we conclude that both glucose and lactate transporter activity is required to sustain CAP activity during EGD when oligodendrocytes are dialyzed with glucose.

DISCUSSION

In white matter, specialized mechanisms for energy delivery are required to maintain axonal function. The axon and its

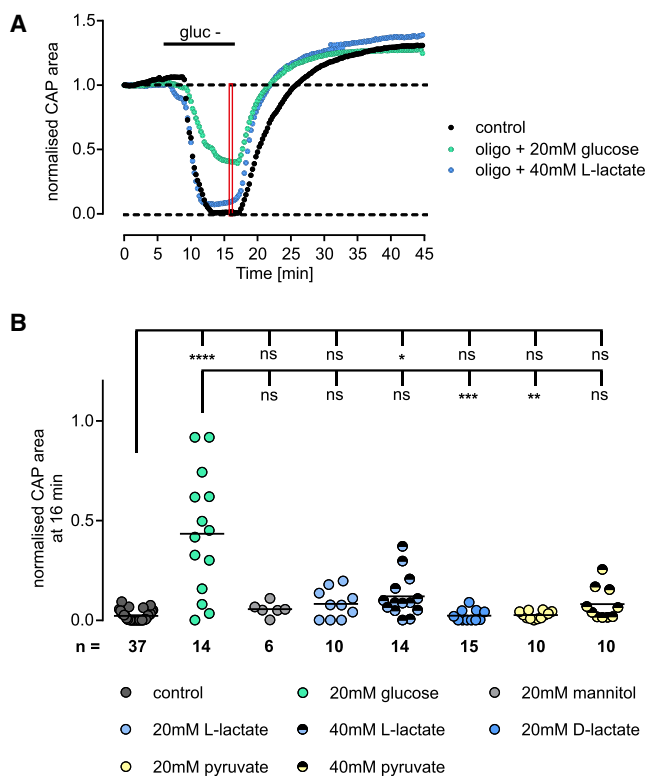


Figure 5. CAP Loss Can Partially Be Prevented during Aglycemia by Filling Oligodendrocytes with Glucose or Equimolar L-Lactate

Top: averaged traces for CAP progression during 10 min of EGD (gluc-) and reperfusion at 36°C without (black) or with preloading of oligodendrocytes with 20 mM glucose (green) or 40 mM L-lactate (blue). Bottom: scatterplots illustrate the normalized CAP area at 16 min (as indicated by the red square in the top graph) shortly before reperfusion. The CAP loss can be significantly prevented only by dialyzing oligodendrocytes with 20 mM glucose or 40 mM L-lactate (40 mM to consider carbon equivalent of 20 mM glucose). Neither 20 mM mannitol, 20 or 40 mM pyruvate, nor the non-metabolizable variant D-lactate prevented CAP loss; control $n = 37$ ($N = 23$), 20 mM mannitol $n = 6$ ($N = 3$), 20 mM glucose $n = 14$ ($N = 10$), 20 mM L-lactate $n = 10$ ($N = 7$), 40 mM L-lactate $n = 14$ ($N = 7$), 20 mM D-lactate $n = 15$ ($N = 9$), 20 mM pyruvate $n = 10$ ($N = 9$), 40 mM pyruvate $n = 10$ ($N = 6$); Kruskal-Wallis test, $p < 0.05$ (black line represents the mean).

enwrapping myelin sheath form a functional unit that enables the exchange of metabolites between oligodendrocytes and axons to meet the high energy demand for action potential generation (Simons and Nave, 2015). In the present study, we investigated axonal activity in the corpus callosum and provide evidence for glucose supply from oligodendrocytes to axons via gap junction-coupled glial networks.

One of our major findings is that in the corpus callosum, CAPs declined within a few minutes after glucose deprivation and, surprisingly, that the replacement of external glucose by L-lactate or pyruvate did not maintain axonal function. Studies of the mechanisms of energy delivery to axons in white matter have so far mostly been performed in the optic nerve, where the transfer of lactate is instrumental to fuel axons (Brown et al., 2003; Fünfschilling et al., 2012). Furthermore, in the absence of glucose and lactate, CAPs in the optic nerve can

be recorded for about 30 min during aglycemia before they fail, indicating that mechanisms of energy storage and supply are different in these brain regions. Indeed, fundamental morphological differences between these two white matter tracts have already been described, particularly regarding the axonal myelination level. Axons in the optic tract are almost completely myelinated (Honjin et al., 1977), whereas myelination in the corpus callosum reaches only 30%–40% and is therefore comparatively sparse (Kim et al., 1996; Mack et al., 1995; Sturrock, 1980). Our immunohistochemical study adds information about the cytoarchitecture of the GFAP-positive astrocytic network in these brain regions. However, it must be noted that there might be overseen GFAP-negative astrocytes and that our quantitative comparison could not yield measures for cell density but rather GFAP-targeted fluorescence signals. Still, it became obvious that the density and spatial arrangement of astrocytes in corpus callosum and optic nerve are different. It is tempting to speculate that these differences could be indicative of a different contribution of astrocytes to the metabolite supply to axons in optic nerve and corpus callosum. Indeed, astrocytes represent the energy storage elements in the brain (Ransom and Fern, 1997; Saab et al., 2013), and in mouse optic nerve, astrocytic glycogen stores were shown to be important to maintain axonal activity. Breakdown of astrocytic glycogen to lactate and lactate shuttling via MCT1 from oligodendrocytes to axons are essential to fuel optic nerve axons during increased neuronal activity and maintain their activity under aglycemic conditions (Brown et al., 2005; Fünfschilling et al., 2012). Thus, in theory, a low glycogen storage capacity of the astrocytic network of the corpus callosum would explain the more rapid decline in the CAP during glucose depletion in our preparation compared with the optic nerve. However, it does not explain the observation that exchange of glucose by L-lactate does not maintain axonal function in the corpus callosum. We therefore conclude that mechanisms of metabolite transport from glial cells to axons in the corpus callosum differ from those in the optic nerve. Indeed, Oe et al. (2016) revealed brain region-dependent differences in glycogen accumulation and suggest metabolic heterogeneity of astrocytes.

In the classic optic nerve preparation, one end of the nerve is stimulated while the activity is recorded at the other end using suction electrodes (Brown et al., 2001). Such an arrangement is not possible in the corpus callosum, and we therefore used acute brain slices, local stimulation, and field potential recordings. This restricted our experiments to a much smaller volume that is within the range of glial networks as determined by biocytin; typically they extend about 200 μm (see Figure 3D). Using a patch-clamp pipette, we then loaded glucose into a single oligodendrocyte in the corpus callosum and found that it can sustain part of the activity of callosal axons when external glucose is withdrawn. Although the infused glucose concentration of 20 mM is far above physiological concentrations of 0.5–1 mM (Saab et al., 2016), such a concentration will most likely only be seen in the soma of the initially patched cell. Glucose concentrations in coupled oligodendrocytes and at the oligodendrocyte compartments close to the axon are hard to predict but will surely be magnitudes lower than 20 mM because of limited diffusion. However, to explain the observed

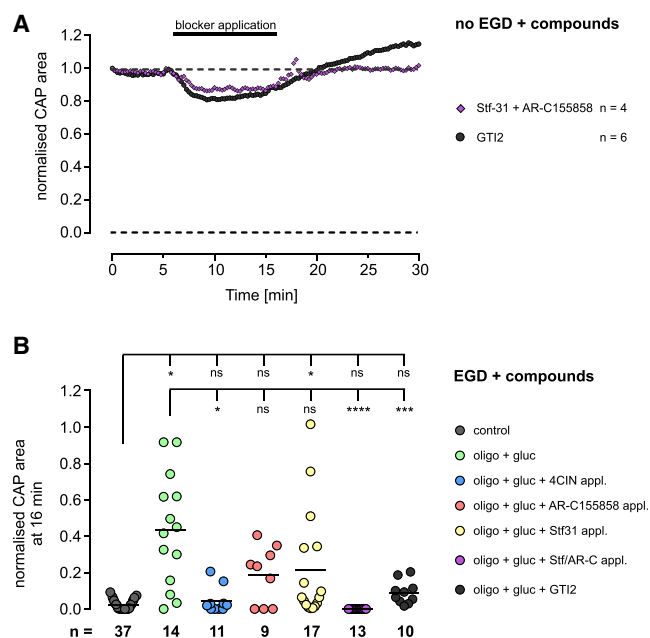


Figure 6. CAP Loss Prevention by Glucose-Loaded Oligodendrocytes Can Be Blocked Only by Combined Disruption of Glucose and Monocarboxylate Transport

(A) Averaged traces for CAP progression during 10 min blocker application while continuously perfusing with glucose-containing ACSF at 36°C with either a combination of Stf31 and AR-C155858 (magenta, $n = 4$, $N = 2$) or GTI2 (dark gray, $n = 6$, $N = 2$). Neither application of 4-CIN, AR-C155858, nor Stf-31 led to a reduction or an overshoot of the measured CAPs.

(B) Pharmacological blockers 4-CIN (200 μ M), AR-C155858 (1 μ M), Stf31 (5 μ M), or GTI2 (5 μ M) were applied simultaneously during EGD. Scatterplot illustrates the normalized CAP area at 16 min (i.e., shortly before glucose reperfusion). CAP loss prevention by previously glucose-filled oligodendrocytes can be abolished only by using the unspecific MCT blocker 4-CIN, by the combination of both specific MCT and GLUT blockers, or by the GLUT3 blocker GTI2. AR-C155858 alone does not affect CAP loss prevention by glucose pre-loading, suggesting that both lactate and glucose are transported to the axons; control $n = 37$ ($N = 23$), glucose filled $n = 14$ ($N = 10$), glucose filled + 4-CIN application $n = 11$ ($N = 5$), glucose filled + AR-C155858 application $n = 9$ ($N = 4$), glucose filled + Stf31 application $n = 17$ ($N = 9$), glucose filled + Stf/AR-C application $n = 13$ ($N = 5$); glucose filled + GTI2 application $n = 10$ ($N = 5$); Kruskal-Wallis test, significant when $p < 0.05$ (black line represents the mean).

rescuing effect during external glucose deprivation, we suppose that glucose levels in the preloaded glial networks are higher compared with networks that were not infused with glucose. Assuming that glucose diffuses at least as well as the larger molecule biocytin, which readily spreads within a coupled glial network in a 200 μ m range, it is most likely that glucose spreads in a similar fashion. The variability in the extent of CAP maintenance during aglycemia after oligodendrocyte filling can likely be explained by the considerable variation in the size of the loaded glial networks after injection into a single oligodendrocyte. This hypothesis is supported by experiments on Cx47KO brain slices in which the smaller glial networks did not support the function of axons during aglycemia. Furthermore, as shown here, longitudinal tracer spread was lower when astrocytes

were injected compared with oligodendrocytes. Moreover astrocytes per se have less direct contact to the axons. These factors may explain why glucose loading of astrocytes failed to rescue axonal activity during aglycemia. However, this observation does not necessarily imply that there is no metabolite support from astrocytes to axons in the corpus callosum at all. It rather indicates that in our experimental paradigm, the rescue of axonal activity during aglycemia largely depends on the integrity of the glucose-loaded oligodendrocyte network between stimulation and field potential recording electrodes. In addition to the discussion above, it is remarkable that glucose application to a single oligodendrocyte reduced the external glucose deprivation-induced loss of CAP amplitude on average to only 40%–50% of the initial control (Figure 2). This percentage is in the range of the population of CAP size from unmyelinated fibers in the corpus callosum (Crawford et al., 2009), and it supports the hypothesis that glucose filling of oligodendrocytes will particularly support the proportion of myelinated axons in our experiments. Unfortunately, with a distance of 300 μ m between stimulation and recording electrode, we could not discriminate between the myelinated and unmyelinated CAP component.

In the present study, we also aimed to identify which metabolite transporters are involved in the energy supply from oligodendrocytes to axons. We focused on members of the glucose transporter (GLUT) family as well as on members of the monocarboxylate transporter family (MCT) that co-transport H^+ and lactate. Although there is evidence that neurons generally prefer lactate over glucose to fuel their energy metabolism (Tekkök et al., 2005), glucose can also be directly taken up and used by neurons in an activity-dependent manner (Lundgaard et al., 2015). Glucose uptake into cells is achieved by a family of integral membrane transporter proteins, the GLUTs. Neurons express primarily GLUT3, whereas GLUT1 is highly enriched in astrocytes and oligodendrocytes (Vannucci et al., 1997; Yu and Ding, 1998). In the optic nerve, GLUT1 was subcellularly detected by immunogold labeling in the myelin sheaths, outer tongue, and paranodal loops of myelinating oligodendrocytes (Saab et al., 2016). GLUT3 is found predominantly in cell processes like the axons (Magnani et al., 1996) and exhibits a lower K_m for glucose uptake and a 5-fold higher capacity for glucose uptake than its glial counterpart GLUT1 (Simpson et al., 2008). This is one possible explanation for the fast recovery of CAPs after aglycemia, as axons might directly take up glucose from the bath and thereby quickly recover their ability to generate action potentials. To explain our experimental aglycemia-rescue paradigm, we first hypothesized that glucose is released from pre-filled oligodendrocytes via GLUT1-mediated export and subsequently imported into the axons and axonal GLUT3-mediated import. Indeed, inhibition of GLUT3 completely abolished CAP rescue during aglycemia; however, in the presence of the GLUT1 inhibitor Stf31, glucose loading of oligodendrocytes still prevented the CAP decline, indicating that mechanisms of energy supply are more complex and involve other elements. In addition, extrusion of glucose via GLUT1 would require glucose-6-phosphatase activity in oligodendrocytes to regenerate glucose after its rapid phosphorylation by hexokinase upon entering the cell. Although glucose-6-phosphatase activity has been shown for cortical oligodendrocytes (Al-Ali and

Robinson, 1981) its expression in callosal oligodendrocytes remains to be proved. One surprising result was that loading of single oligodendrocytes with high concentrations of lactate (40 mM) did, like glucose, support axonal CAPs during aglycemia. This indicates lactate transport between neurons and oligodendrocytes. One reason for a less effective rescuing effect by loading lactate compared with glucose into glial networks may be that the diffusion of lactate into the oligodendrocyte processes is hampered by its negative charge and electrostatic interactions with numerous binding sites in the cytoplasm. Inhibition of the oligodendroglial MCT1 and axonal MCT2 lactate transporters during aglycemia did not abolish glucose support from oligodendrocytes. However, the combined blockade of oligodendroglial lactate and glucose export using MCT1/2 and GLUT1 inhibitors completely abolished the oligodendroglial support to axons during aglycemia, indicating that there must be both glucose and lactate supply from oligodendrocyte to axons via MCTs and GLUT1. Also, it remains elusive why blockade of axonal GLUT3 successfully prevented metabolic support from oligodendrocytes during aglycemia, and the experiments performed in the present study cannot give a conclusive answer to that question. We therefore conclude that the panglial network in the corpus callosum is important for metabolic support of axons, and that oligodendroglial supply of lactate and glucose via MCT1 and GLUT1 must be a major component of its underlying mechanism.

EXPERIMENTAL PROCEDURES

Animals and Handling

All procedures involving handling of living animals were performed in accordance with the German Animal Protection Law and were approved by the Regional Office for Health and Social Services in Berlin (Landesamt für Gesundheit und Soziales, Berlin, Germany, approval T0014/08, X9023/12).

Transgenic PLP-GFP (Fuss et al., 2000) and GFAP-mRFP (Hirrlinger et al., 2005) reporter mice and Cx47-deficient mice (Tress et al., 2012) of either sex, aged 28–35 days, were used for the studies. For preparation of acute brain slices, mice were sacrificed by cervical dislocation as described by (Maglione et al., 2010) and as detailed in Supplemental Experimental Procedures. For immunohistochemistry, mice were sacrificed by deep anesthesia and perfusion fixation. All efforts were made to minimize suffering.

Recording of CAPs and External Glucose Deprivation

Extracellular field potentials were recorded at room temperature or 36°C in freshly prepared brain slices that were placed in a recording chamber mounted on an upright microscope as previously described (Richter et al., 2014). Stimulation and recording electrodes (impedance 100–500 k Ω) were placed in the corpus callosum both about 150 μ m lateral of the midline (Figure 1A). The stimulation protocol and analysis of the evoked CAP is detailed in Supplemental Experimental Procedures.

For EGD experiments at 36°C, the perfusion with glucose-containing ACSF was switched for 10 min to glucose-free ACSF, before the slice was reperfused with glucose-containing ACSF for 30 min. In experiments at room temperature, the EGD period lasted for 55 min. In some experiments, glucose was replaced by L-lactate, D-lactate, pyruvate, or mannitol. Pharmacological blockers of lactate and glucose transporters 4-CIN, AR-C155858, Stf31, and GTI2 and were applied via the bath perfusion.

Patch-Clamp Recordings

Oligodendrocytes (PLP-GFP) in the corpus callosum were identified by their GFP fluorescence and astrocytes in hGFAP-mRFP mice by their RFP fluorescence, using a 60 \times water-immersion objective. For recording and metabolic

loading, a patch pipette was pulled from borosilicate glass and filled with a HEPES-buffered intracellular solution to which we added 20 mM glucose, 20 mM mannitol, 20 mM L-lactate, 40 mM D-lactate, 20 mM D-lactate, 20 mM pyruvate, or 40 mM pyruvate. Sulforhodamine B (10 μ g/mL) was added to the pipette solution for confirmation of intracellular access during the patch-clamp experiment. The pipette resistance ranged from 4 to 7 M Ω . Cells were selected close to the stimulation electrode ensuring that the stimulated axons were in proximity to the potential glucose-filled panglial network. Cells were dialyzed via the patch pipette for 20 min prior to EGD to ensure that the metabolites spread into coupled cells of the panglial network. To confirm the cell identity and vitality, membrane currents were recorded as described previously (Richter et al., 2014). Only cells that showed a series resistance \leq 125% at the end of the dialysis process compared with the start were taken into account for the calculation of the membrane properties. After metabolite loading and patch-clamp recording, the pipette was carefully removed from the cell in order to disrupt the patch. Specifications and details of the analysis of the recordings are given in Supplemental Experimental Procedures.

Dye-Coupling Experiments, Immunohistochemistry, and Quantification

Characterization of coupled networks in the corpus callosum was performed by dye filling, subsequent immunohistochemistry, and confocal microscopy in acute brain slices of mice aged 28–35 days as previously described (Maglione et al., 2010). GFAP immunohistochemistry on cryosections of corpus callosum and optic nerve was done as described previously (Nolte et al., 2001) with modifications. Details and information on quantification are given in Supplemental Experimental Procedures.

Statistics

Results were statistically analyzed using Graph Pad Prism Software (La Jolla, CA 92037 USA). If not otherwise stated data are provided as mean \pm SEM; n refers to the number of brain slices investigated and N to the number of animals. These numbers are indicated in the figure legends and in the text. Data were tested using Student's two-tailed t test or the Kruskal-Wallis test. Differences were regarded as significant at *p < 0.05, **p < 0.01, ***p < 0.001, or ****p < 0.0001.

SUPPLEMENTAL INFORMATION

Supplemental Information includes Supplemental Experimental Procedures and five figures and can be found with this article online at <https://doi.org/10.1016/j.celrep.2018.02.022>.

ACKNOWLEDGMENTS

We are grateful to Nadine Scharek, Michaela Seeger-Zografakis, and the Advanced Light Microscopy facility at the Max Delbrueck Center for Molecular Medicine, Berlin-Buch for technical assistance, the German Research Foundation (KE 329/28, STE 552/4) for financial support, and the medical neuroscience graduate program of Charité Berlin.

AUTHOR CONTRIBUTIONS

Conceptualization, H.K. and C.S.; Methodology, N.M. and N.R.; Investigation, N.M., C.N., N.R., Z.F., G.S., and T.P.; Software, P.J.; Supervision, C.N., C.S., M.S., and H.K.; Writing – Original Draft, N.M., C.N., C.S., and H.K.; Writing – Review & Editing, N.M., N.R., Z.F., G.S., T.P., C.S., M.S., C.N., and H.K.; Funding Acquisition, H.K. and C.S.

DECLARATION OF INTERESTS

The authors declare no competing interests.

Received: July 27, 2017

Revised: January 12, 2018

Accepted: February 5, 2018

Published: February 27, 2018

REFERENCES

- Al-Ali, S.Y., and Robinson, N. (1981). Ultrastructural demonstration of glucose 6-phosphatase in cerebral cortex. *Histochemistry* 72, 107–111.
- Berger, T., Schnitzer, J., and Kettenmann, H. (1991). Developmental changes in the membrane current pattern, K⁺ buffer capacity, and morphology of glial cells in the corpus callosum slice. *J. Neurosci.* 11, 3008–3024.
- Brown, A.M., Wender, R., and Ransom, B.R. (2001). Metabolic substrates other than glucose support axon function in central white matter. *J. Neurosci. Res.* 66, 839–843.
- Brown, A.M., Tekkök, S.B., and Ransom, B.R. (2003). Glycogen regulation and functional role in mouse white matter. *J. Physiol.* 549, 501–512.
- Brown, A.M., Sickmann, H.M., Fosgerau, K., Lund, T.M., Schousboe, A., Waagepetersen, H.S., and Ransom, B.R. (2005). Astrocyte glycogen metabolism is required for neural activity during aglycemia or intense stimulation in mouse white matter. *J. Neurosci. Res.* 79, 74–80.
- Crawford, D.K., Mangiardi, M., and Tiwari-Woodruff, S.K. (2009). Assaying the functional effects of demyelination and remyelination: revisiting field potential recordings. *J. Neurosci. Methods* 182, 25–33.
- Fünfschilling, U., Supplie, L.M., Mahad, D., Boretius, S., Saab, A.S., Edgar, J., Brinkmann, B.G., Kassmann, C.M., Tzvetanova, I.D., Möbius, W., et al. (2012). Glycolytic oligodendrocytes maintain myelin and long-term axonal integrity. *Nature* 485, 517–521.
- Fuss, B., Mallon, B., Phan, T., Ohlemeyer, C., Kirchhoff, F., Nishiyama, A., and Macklin, W.B. (2000). Purification and analysis of in vivo-differentiated oligodendrocytes expressing the green fluorescent protein. *Dev. Biol.* 218, 259–274.
- Griemsmann, S., Höft, S.P., Bedner, P., Zhang, J., von Staden, E., Beinhauer, A., Degen, J., Dublin, P., Cope, D.W., Richter, N., et al. (2015). Characterization of Panglial gap junction networks in the thalamus, neocortex, and hippocampus reveals a unique population of glial cells. *Cereb. Cortex.* 25, 3420–3433.
- Hirrlinger, P.G., Scheller, A., Braun, C., Quintela-Schneider, M., Fuss, B., Hirrlinger, J., and Kirchhoff, F. (2005). Expression of reef coral fluorescent proteins in the central nervous system of transgenic mice. *Mol. Cell. Neurosci.* 30, 291–303.
- Hof, P.R., Pascale, E., and Magistretti, P.J. (1988). K⁺ at concentrations reached in the extracellular space during neuronal activity promotes a Ca²⁺-dependent glycogen hydrolysis in mouse cerebral cortex. *J. Neurosci.* 8, 1922–1928.
- Honjin, R., Sakato, S., and Yamashita, T. (1977). Electron microscopy of the mouse optic nerve: a quantitative study of the total optic nerve fibers. *Arch. Histol. Jpn.* 40, 321–332.
- Kim, J.H., Ellman, A., and Juraska, J.M. (1996). A re-examination of sex differences in axon density and number in the splenium of the rat corpus callosum. *Brain Res.* 740, 47–56.
- Lee, Y., Morrison, B.M., Li, Y., Lengacher, S., Farah, M.H., Hoffman, P.N., Liu, Y., Tsingalia, A., Jin, L., Zhang, P.W., et al. (2012). Oligodendroglia metabolically support axons and contribute to neurodegeneration. *Nature* 487, 443–448.
- Lundgaard, I., Li, B., Xie, L., Kang, H., Sanggaard, S., Haswell, J.D., Sun, W., Goldman, S., Bleköt, S., Nielsen, M., et al. (2015). Direct neuronal glucose uptake heralds activity-dependent increases in cerebral metabolism. *Nat. Commun.* 6, 6807.
- Mack, C.M., Boehm, G.W., Berrebi, A.S., and Denenberg, V.H. (1995). Sex differences in the distribution of axon types within the genu of the rat corpus callosum. *Brain Res.* 697, 152–160.
- Maglione, M., Tress, O., Haas, B., Karam, K., Trotter, J., Willecke, K., and Kettenmann, H. (2010). Oligodendrocytes in mouse corpus callosum are coupled via gap junction channels formed by connexin47 and connexin32. *Glia* 58, 1104–1117.
- Magnani, P., Cherian, P.V., Gould, G.W., Greene, D.A., Sima, A.A., and Brosius, F.C., 3rd. (1996). Glucose transporters in rat peripheral nerve: paranodal expression of GLUT1 and GLUT3. *Metabolism* 45, 1466–1473.
- Morrison, B.M., Lee, Y., and Rothstein, J.D. (2013). Oligodendroglia: metabolic supporters of axons. *Trends Cell Biol.* 23, 644–651.
- Nave, K.A., and Werner, H.B. (2014). Myelination of the nervous system: mechanisms and functions. *Annu. Rev. Cell Dev. Biol.* 30, 503–533.
- Nolte, C., Matyash, M., Pivneva, T., Schipke, C.G., Ohlemeyer, C., Hanisch, U.K., Kirchhoff, F., and Kettenmann, H. (2001). GFAP promoter-controlled EGFP-expressing transgenic mice: a tool to visualize astrocytes and astroglia in living brain tissue. *Glia* 33, 72–86.
- Odermatt, B., Wellershaus, K., Wallraff, A., Seifert, G., Degen, J., Euwens, C., Fuss, B., Büssow, H., Schilling, K., Steinhäuser, C., and Willecke, K. (2003). Connexin 47 (Cx47)-deficient mice with enhanced green fluorescent protein reporter gene reveal predominant oligodendrocytic expression of Cx47 and display vacuolized myelin in the CNS. *J. Neurosci.* 23, 4549–4559.
- Oe, Y., Baba, O., Ashida, H., Nakamura, K.C., and Hirase, H. (2016). Glycogen distribution in the microwave-fixed mouse brain reveals heterogeneous astrocytic patterns. *Glia* 64, 1532–1545.
- Ransom, B.R., and Fern, R. (1997). Does astrocytic glycogen benefit axon function and survival in CNS white matter during glucose deprivation? *Glia* 21, 134–141.
- Reyes-Haro, D., Mora-Loyola, E., Soria-Ortiz, B., and García-Colunga, J. (2013). Regional density of glial cells in the rat corpus callosum. *Biol. Res.* 46, 27–32.
- Richter, N., Wendt, S., Georgieva, P.B., Hambardzumyan, D., Nolte, C., and Kettenmann, H. (2014). Glioma-associated microglia and macrophages/monocytes display distinct electrophysiological properties and do not communicate via gap junctions. *Neurosci. Lett.* 583, 130–135.
- Rouach, N., Koulakoff, A., Abudara, V., Willecke, K., and Giaume, C. (2008). Astroglial metabolic networks sustain hippocampal synaptic transmission. *Science* 322, 1551–1555.
- Saab, A.S., Tzvetanova, I.D., and Nave, K.A. (2013). The role of myelin and oligodendrocytes in axonal energy metabolism. *Curr. Opin. Neurobiol.* 23, 1065–1072.
- Saab, A.S., Tzvetanova, I.D., Trevisiol, A., Baltan, S., Dibaj, P., Kusch, K., Möbius, W., Goetze, B., Jahn, H.M., Huang, W., et al. (2016). Oligodendroglial NMDA receptors regulate glucose import and axonal energy metabolism. *Neuron* 91, 119–132.
- Simons, M., and Nave, K.A. (2015). Oligodendrocytes: myelination and axonal support. *Cold Spring Harb. Perspect. Biol.* 8, a020479.
- Simpson, I.A., Dwyer, D., Malide, D., Moley, K.H., Travis, A., and Vannucci, S.J. (2008). The facilitative glucose transporter GLUT3: 20 years of distinction. *Am. J. Physiol. Endocrinol. Metab.* 295, E242–E253.
- Sotelo-Hitschfeld, T., Niemeyer, M.I., Mächler, P., Ruminot, I., Lerchundi, R., Wyss, M.T., Stobart, J., Fernández-Moncada, I., Valdebenito, R., Garrido-Gerter, P., et al. (2015). Channel-mediated lactate release by K⁺-stimulated astrocytes. *J. Neurosci.* 35, 4168–4178.
- Sturrock, R.R. (1980). Myelination of the mouse corpus callosum. *Neuropathol. Appl. Neurobiol.* 6, 415–420.
- Sun, D., Lye-Barthel, M., Masland, R.H., and Jakobs, T.C. (2009). The morphology and spatial arrangement of astrocytes in the optic nerve head of the mouse. *J. Comp. Neurol.* 516, 1–19.
- Tekkök, S.B., Brown, A.M., Westenbroek, R., Pellerin, L., and Ransom, B.R. (2005). Transfer of glycogen-derived lactate from astrocytes to axons via specific monocarboxylate transporters supports mouse optic nerve activity. *J. Neurosci. Res.* 81, 644–652.
- Tress, O., Maglione, M., Zlomuzica, A., May, D., Dicke, N., Degen, J., Dere, E., Kettenmann, H., Hartmann, D., and Willecke, K. (2011). Pathologic and phenotypic alterations in a mouse expressing a connexin47

missense mutation that causes Pelizaeus-Merzbacher-like disease in humans. *PLoS Genet.* 7, e1002146.

Tress, O., Maglione, M., May, D., Pivneva, T., Richter, N., Seyfarth, J., Binder, S., Zlomuzica, A., Seifert, G., Theis, M., et al. (2012). Panglial gap junctional communication is essential for maintenance of myelin in the CNS. *J. Neurosci.* 32, 7499–7518.

Trotter, J., Karram, K., and Nishiyama, A. (2010). NG2 cells: properties, progeny and origin. *Brain Res. Rev.* 63, 72–82.

Vannucci, S.J., Maher, F., and Simpson, I.A. (1997). Glucose transporter proteins in brain: delivery of glucose to neurons and glia. *Glia* 21, 2–21.

Yu, S., and Ding, W.G. (1998). The 45 kDa form of glucose transporter 1 (GLUT1) is localized in oligodendrocyte and astrocyte but not in microglia in the rat brain. *Brain Res.* 797, 65–72.